10TH INTERNATIONAL SYMPOSIUM ON PARTICLE IMAGE VELOCIMETRY - PIV13
Delft, The Netherlands, July 1-3, 2013

Methods for estimating higher order moments from PIV data

Sven Scharnowski and Christian J. Kähler

Institute of Fluidmechanics and Aerodynamics
Bundeswehr University Munich, Werner-Heisenberg-Weg 39, 85577 Neubiberg, Germany
sven.scharnowski@unibw.de

ABSTRACT

This work shows how the probability density function (PDF) of the turbulent velocity fluctuation can be estimated from the deconvolution of ensemble averaged cross-correlation and auto-correlation functions of PIV recordings. Once the PDF is known, the mean displacement, the Reynolds stresses as well as higher order moments can reliable be estimated. The approach was tested on synthetic PIV images and the results are compared to those obtained by standard window correlation as well as by deconvolution of Gaussian fit functions. The effect of the number of images pairs, the digital particle image size, and the shape of the PDF on the random error of the estimated moments was investigated. It was found that the developed method can also handle complex shaped PDF's like an asymmetric peak or two separated peaks. The new approach is also applied to evaluate an experimental data set in order to demonstrate its suitability for real flows.

1. INTRODUCTION

PIV has become a well established measurement technique for non-intrusive determination of velocity distributions in transparent fluids. Due to the two-dimensional or three-dimensional results, this measurement technique reveals fundamental information about turbulent structures which could not be analyzed with point-wise methods like hot wire anemometers or laser Doppler anemometers. Besides instantaneous velocity fields, PIV also allows for the determination of flow statistics like the mean velocity distribution or Reynolds stress distributions. Such flow statistics are very important for the comparison of different experiments or for the validation of numerical methods. For a sufficient number of statistically independent velocity fields the mean velocity components $\langle u_\mathrm{i} \rangle$, the Reynolds stresses $\langle u'_\mathrm{i} \cdot u'_\mathrm{j} \rangle$ and higher order moments, such as $\langle u'_\mathrm{i} \cdot u'_\mathrm{j} \cdot u'_\mathrm{k} \rangle$, can be determined from the individual velocity fields $\vec{u}_\mathrm{n}(\vec{x})$:

$$\left\langle u'_\mathrm{i} \cdot u'_\mathrm{j} \cdot \ldots \right\rangle = \quad \frac{1}{N} \sum_{\mathrm{n}=1}^{N} \left(u_{\mathrm{i,n}} - \langle u_\mathrm{i} \rangle \right) \cdot \left(u_{\mathrm{j,n}} - \langle u_\mathrm{j} \rangle \right) \cdot \ldots \tag{1}$$

Where the mean velocity components $\langle u_\mathrm{i} \rangle$ are computed as follows:

$$\langle u_\mathrm{i} \rangle = \frac{1}{N} \sum_{\mathrm{n}=1}^{N} u_{\mathrm{i,n}} \tag{2}$$

N and *n* are the total number of vector fields and the corresponding control variable, respectively. All statistics computed from Eq. 1 have the same spatial resolution as the original vector fields. Thus, in the case of strong gradients combined with insufficient spatial resolution, the results are biased. Furthermore, the results are spatially low-pass filtered due to the finite interrogation-window size, as discussed in detail in [4] and [8]. In order to improve the spatial resolution and to overcome the fundamental problem of low-pass filtering, ensemble-correlation PIV evaluation [6, 11] combined with correlation-peak analysis methods [1, 2, 8, 10] can be applied to determine the velocity's PDF. The authors have shown that the mean velocity and Reynolds stresses can be more precisely estimated from the PDF rather than from an ensemble of velocity vector fields [8]:

$$\left\langle u'_\mathrm{i} \cdot u'_\mathrm{j} \cdot \ldots \right\rangle = \int \mathrm{PDF} \cdot \left(u'_\mathrm{i} \cdot u'_\mathrm{j} \cdot \ldots \right) \mathrm{d}\vec{u} \tag{3}$$

The question, which is in the focus of this work, is: How can the PDF reliably be determined from the correlation function in order to estimate higher order moments? To answer this question, two different methods for estimating the PDF are discussed in Sec. 2. Sections 3 illustrate the application of these methods for the evaluation of synthetic PIV data and compares the results with those of standard window correlation methods based on Eq. 1. It will be shown that the direct deconvolution of the cross-correlation function with the auto-correlation function results in reliable values for higher order moments. Section 4 analyzes the effect of different parameters on the accuracy of the estimated moments and Sec. 5 demonstrates the suitability of the developed approach for the evaluation of experimental PIV data.

2. ESTIMATING THE VELOCITY'S PROBABILITY DENSITY FUNCTION

Ensemble-correlation PIV evaluation methods, like averaged window-correlation [6] or single-pixel ensemble-correlation [11] are well suited to determine the two-dimensional mean velocity distribution with high spatial resolution. On the other hand, these techniques do not yield instantaneous vector fields, from which statistics can be estimated. Thus, Eq. 1 and 2 cannot be applied. Several works, including [1, 2, 8, 10], showed that the velocity's probability density function is trapped in the ensemble-averaged correlation function. Since the correlation function C is the convolution (indicated by $\otimes$) of the PDF and the auto-correlation function R

$$C = R \otimes \mathrm{PDF} \tag{4}$$

the deconvolution of C with R yields the PDF, theoretically.

One approach to determine the PDF is to approximate R and C by fit functions and to perform the deconvolution analytically. Using Gaussian functions for R and C with circular and elliptical cross sections, respectively, allows for the reconstruction of the PDF with relatively low mathematical effort. This approach is well suited to estimate Reynolds stresses, as outlined in [8]. For a Gaussian PDF with an elliptical cross section (major axis P_X, minor axis P_Y) and an angle of rotation α

$$PDF = \frac{8}{\pi \cdot P_\mathrm{X} \cdot P_\mathrm{Y}} \cdot \quad \exp\left[-\left(\frac{\cos\alpha \cdot (X-\Delta X) - \sin\alpha \cdot (Y-\Delta Y)}{P_\mathrm{X}} \right)^2 \cdot 8 - \left(\frac{\sin\alpha \cdot (X-\Delta X) + \cos\alpha \cdot (Y-\Delta Y)}{P_\mathrm{Y}} \right)^2 \cdot 8 \right] \tag{5}$$

the Reynolds stresses can be calculated from

$$\left\langle u'^2 \right\rangle = \frac{1}{16} \cdot \left(\cos^2\alpha \cdot p_\mathrm{x}^2 + \sin^2\alpha \cdot p_\mathrm{y}^2 \right), \tag{6}$$

$$\left\langle v'^2 \right\rangle = \frac{1}{16} \cdot \left(\sin^2\alpha \cdot p_\mathrm{x}^2 + \cos^2\alpha \cdot p_\mathrm{y}^2 \right), \tag{7}$$

and

$$\left\langle u' \cdot v' \right\rangle = \left\langle v' \cdot u' \right\rangle = \frac{1}{16} \cdot \cos\alpha \cdot \sin\alpha \left(p_\mathrm{y}^2 - p_\mathrm{x}^2 \right), \tag{8}$$

as discussed in detail in [8]. Where $P_{\mathrm{X,Y}}$ and $p_{\mathrm{x,y}}$ are the PDF's cross section parameters on the image plane and on the measurement plane, respectively. The major difficulty of this method is that it requires prior knowledge about the PDF. Using complex fit functions can lead to a good representation of the correlation functions, but it might also result in mathematically challenges for the analytical deconvolution or even in ill-posed problems. The Gaussian with elliptical cross section is a compromise between complexity and suitability, which works well for the estimation of Reynolds stresses.

Another approach to extract the PDF is the direct deconvolution of the discrete correlation functions R and C. In order to find the best approximation for the discrete PDF, the sum of squared errors (SSE)

$$\mathrm{SSE} = \sum_{\Delta\mathrm{X}} \sum_{\Delta\mathrm{Y}} (R \otimes \mathrm{PDF} - C)^2 \tag{9}$$

must be minimized. Since the probability is larger or equal zero for all velocities,

$$\mathrm{PDF} \geq 0 \qquad \text{for all } \Delta X, \Delta Y \tag{10}$$

this physical condition is used in the optimization procedure. Figure 1 shows an example for the cross-correlation function, the corresponding auto-correlation function and the estimated PDF. From the discrete PDF higher order moments can be extracted as follows:

$$\left\langle u'_\mathrm{i} \cdot u'_\mathrm{j} \cdot \ldots \right\rangle = \sum_\mathrm{u} \sum_\mathrm{v} \mathrm{PDF} \cdot \left(u'_\mathrm{i} \cdot u'_\mathrm{j} \cdot \ldots \right) \tag{11}$$

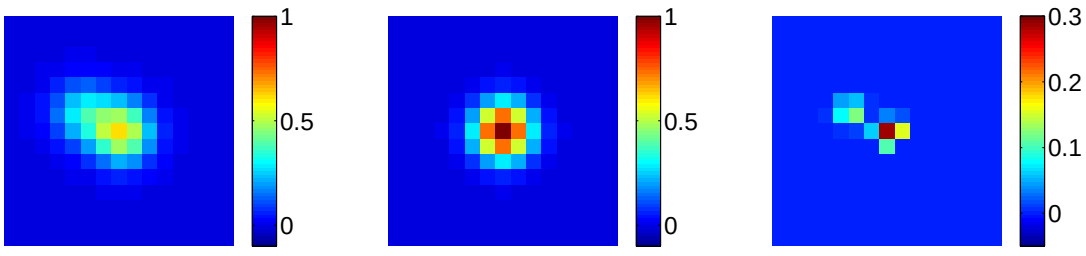

(a) (b) (c)

Figure 1: Example of a cross-correlation function (a) and a corresponding auto-correlation function (b) computed from synthetic PIV images using ensemble-averaged window correlation. The PDF is estimated via direct deconvolution of the discrete functions (c).

The major advantage of this approach is that any shape of the PDF can be reconstructed without previous knowledge about it. The method works for an unsymmetrical PDF as well as for a PDF with separated peaks, as will be demonstrated in the following sections.

3. SYNTHETIC EXAMPLE

The estimation of the mean displacement, the Reynolds stresses and higher moments is now applied to synthetic PIV images. Only synthetic data gives full control of all relevant parameters, as discussed in detail in [5]. Therefore, this examination is a necessary step for the validation of the developed approach.

In order to analyze the capability to estimate higher order moments an asymmetric PDF was simulated. $10,000$ PIV image pairs, 1024×1024 px in size, were generated. The maximum intensity of individual particle images and the signal to noise ration were 2^{14} and $100:1$, respectively. The simulated digital particle image diameter D, which is defined as the full width at $1/e^2$ of the maximum intensity (4 times the standard deviation), varies from left to right while the shape of the PDF changes from top to bottom. The fraction of illuminated area was set to 25%, corresponding to 0.08 or 0.02 particle images per pixel for $D = 2$ or 4 px, respectively. To account for the discrete nature of digital images, the intensity for each pixel of the particle images was computed from an integral over the pixel size, as discussed in [9]. The pixel size, on the other hand, was assumed to be equal to the pixel grid spacing, simulating a sensor fill factor of 1.

A PDF consisting of two Gaussian was simulated. Both have a circular cross section and a diameter (4 times the standard deviation) of $p = 2.5$ px, one Gaussian is centered at $(\Delta X, \Delta Y) = (0,0)$ and the second one is located at $(\Delta X, \Delta Y) = (s, s/2)$. The probability of the first Gaussian is twice as high as for the second one. The parameter s varies from -5 at the top of the images to $+5$ at the bottom of the images, whilde D changes from 1 px at the left side to 5 px at the right side of the images. Figure 2 shows different simulated PDF's and the corresponding cross-correlation functions for two different digital particle image diameters. The correlation functions were computed from averaged window-correlation using a commercial software (DaVis by LaVision) with a interrogation window size of 16×16 px and 50% overlap.

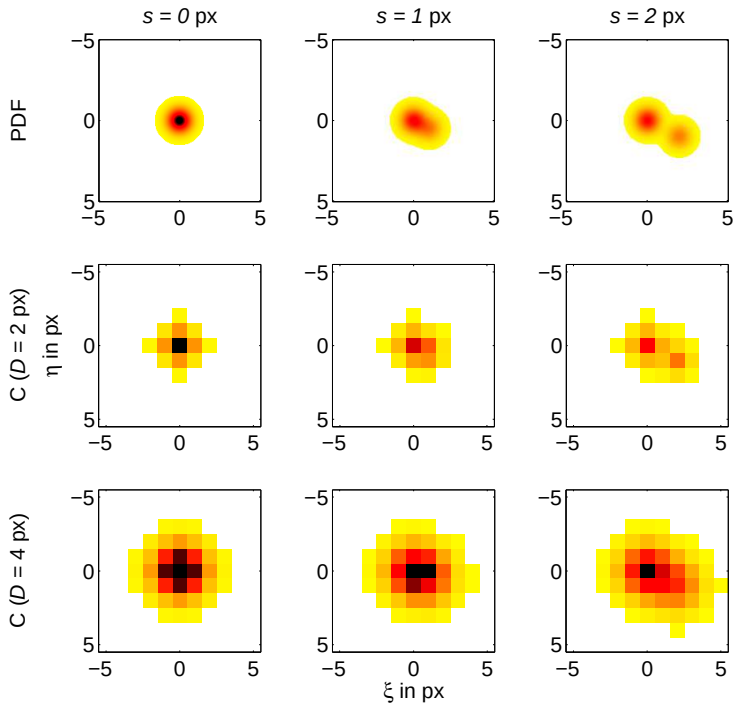

Figure 2: Synthetic test case with varying PDF and particle image size. Top row: different simulated PDF's. Middle and bottom row: cross-correlation function for a digital particle image diameter of $D = 2$ px and $D = 4$ px, respectively.

The results for the estimated horizontal mean displacement, the in plane Reynolds stresses and exemplary higher order moments are shown in Fig. 3. The sub-figures show the comparison between the deconvolution of the discrete functions R and C, the deconvolution of Gaussian fit functions as well as the results of standard window correlation. Since individual particle images in the synthetic PIV images were uncorrelated, the simulated turbulent structures are infinitely small in size. Due to this, the window correlation approach acts as a low-pass filter and leads to an underestimation of the velocity fluctuations, as discussed in [8]. Furthermore, since only the highest correlation value is cosidered even the mean displacement is biased for a peak separation $|s| > 1$ px.

The Gaussian fit function combined with the analytical deconvolution is well suited to estimate the mean displacement and the Reynolds stresses in the case of small peak separation ($s < 3$ px). However, as soon as the peaks in the cross-correlation function start to separate, the estimation of all statistics is strongly biased. Furthermore, due to the symetry of the fit function some moments ($\langle u'^3 \rangle$, $\langle u'^2 \cdot v' \rangle$, ...) are always estimated to be zero.

The deconvolution of the discrete cross-correltation and auto-correlation function is the only tested approach that can handle a PDF with separated peaks. The mean displacement, the Reynolds stresses as well as higher order moments are estimated without significant bias errors, as can be seen from the results in Fig. 3.

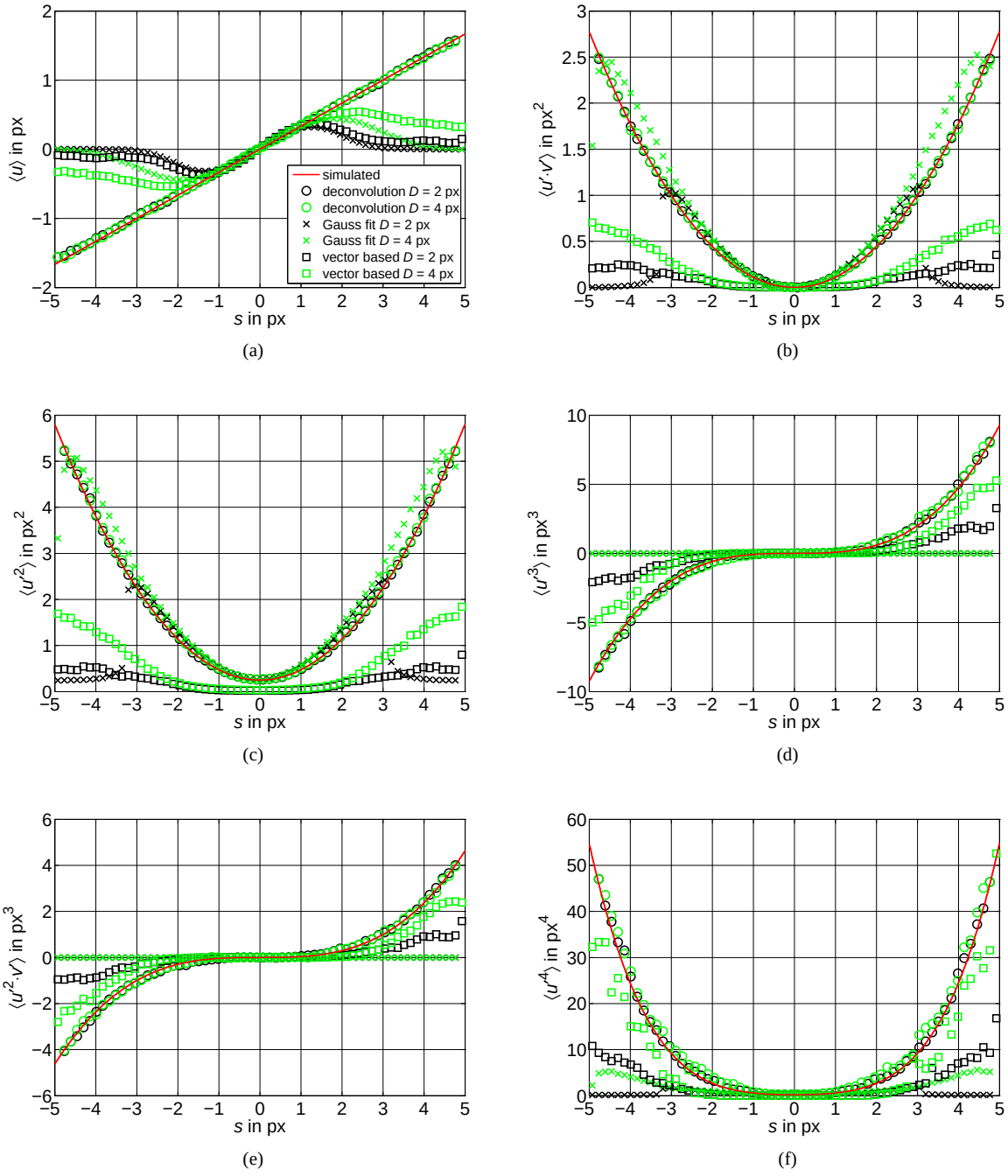

Figure 3: Moments of different orders estimated with the proposed deconvolution method, from the deconvolution of Gaussian fit functions, and from instantaneous velocity fields. The simulated values are indicated by the red solid line.

4. PARAMETERS THAT EFFECT THE UNCERTAINTY OF THE PDF ESTIMATION

In the previous section it was shown that the direct deconvolution of the cross-correlation function and the auto-correlation function allows for the estimation of the PDF and thus, for higher order moments. In order to analyze the sensitivity of this new approach, more synthetic PIV images with varying properties were generated and evaluated.

The first parameter which was altered is the number of image pairs. A total number of $100,000$ image pairs, 128×128 px in size, with a digital particle image diameter of $D = 2$ px was generated. The simulated PDF consist again of two Gaussian and was constant over the image area. Both Gaussian have a diameter of $p = 2.5$ px, one is centered at $(\Delta X, \Delta Y) = (0,0)$ and the second one is located at

$(\Delta X, \Delta Y) = (2.5\,\mathrm{px}, 1.25\,\mathrm{px})$. The probability of the first Gaussian is twice as high as for the second one. The cross correlation and the auto correlation were computed with averaged window correlation by using again a commercial software (DaVis by LaVision) for a subset of the images and the deconvolution was applied to the discrete functions. The interrogation windows were 16×16 px in size with 50% overlap. Figure 4 shows the relative standard deviation of estimated moments (normalized with the simulated values) with respect to the number of image pairs. As expected, the random error decreases with increasing number of images. It can be seen that the higher the order of the estimated moment the more images are required in order to achieve the same accuracy. While 100 double images are sufficient to estimate $\langle u' \cdot v' \rangle$ with an random error of 5% for the tested interrogation-window size, more than $1,000$ image pairs are needed to estimate $\langle u'^4 \rangle$ with 5% random error.

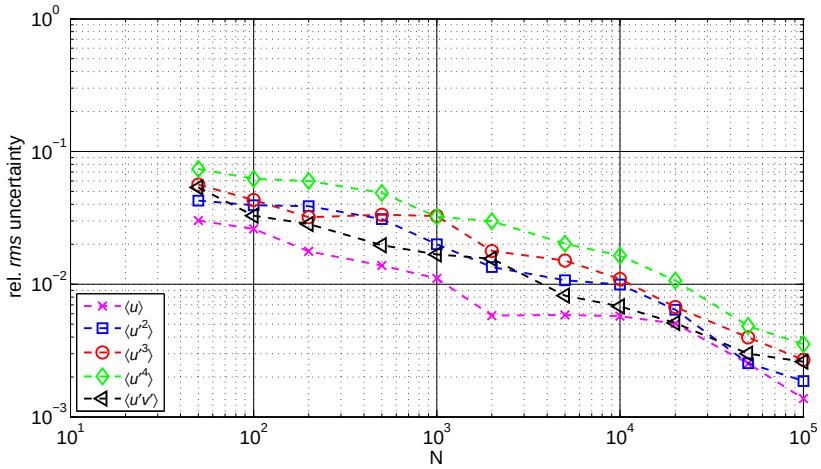

Figure 4: Effect of the number of synthetic image pairs on the rms uncertainty of the estimated moments of different orders.

The second tested parameter is the digital particle image diameter D. Another set of $10,000$ synthetic images, 1024×1024 px in size, was generated: The simulated PDF was constant over the image area and consists of two Gaussian as before. The particle image size was varied from left to right from 1.5 px up to 10 px. The illuminated area was constant (25%) causing a reduced number of particle images for regions with larger D. Figure 5 shows the estimated standard deviation normalized with the simulated values for different moments. It can be seen that the random error increases with increasing particle image size. Thus, D should be between 1.5 px and 5 px in order to achieve reliable results.

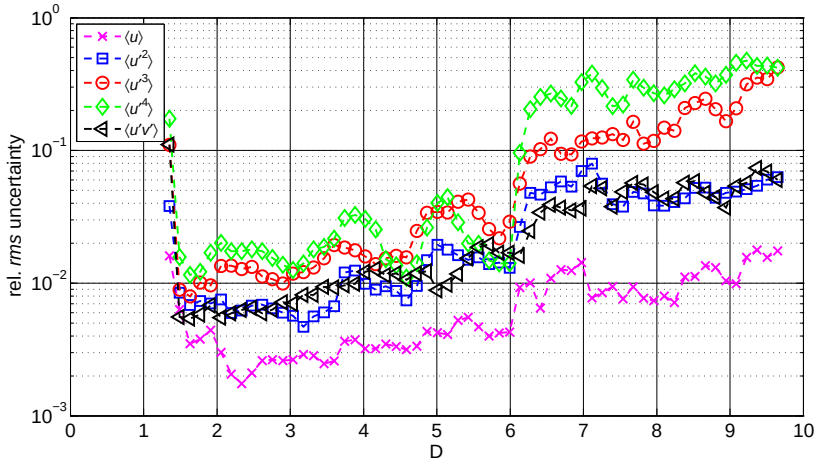

Figure 5: Effect of the digital particle image diameter D of synthetic images on the rms uncertainty of the estimated moments of different orders.

Another important parameter, which was investigated, is the shape of the PDF. A set of $10,000$ synthetic images, 1024×1024 px in size, was generated: The simulated PDF consists of two Gaussian separated by 2.5 px in horizontal and 1.25 px in vertical direction, as before. However, the diameter p of the Gaussian varied from left to right between 0 px and 5 px. A particle image size of $D = 2$ px was simulated. The results are summarized in Fig. 6: The higher the order of the estimated moment the larger is the random error, as before. Furthermore, the accuracy is best for a PDF with small diameter p.

In summary, higher order moments can be estimated for all tested parameter variations. The best results are achieved for a PDF with two Gaussian of small diameter ($p < 1$ px) and small particle images ($1.5 < D < 5$). In the case of larger p or D, the number of image pairs can be increased to achieve comparable accuracy.

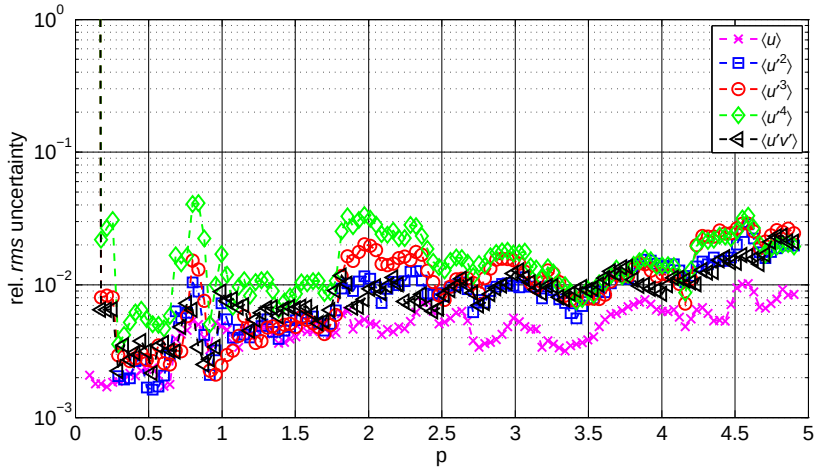

Figure 6: Effect of the shape of the PDF of synthetic images on the rms uncertainty of the estimated moments of different orders.

5. EXPERIMENTAL EXAMPLE

In order demonstrate the suitability of the developed approach for experimental PIV images, a real flow experiment over periodic hills was analyzed. The experiments were performed in a water tunnel at TU Munich at a Reynolds number of $\mathrm{Re_h} = 8,000$, based on the hill height. Details about the setup can be found in [3] and [7]. The results in Fig. 7 were estimated from the shape of sum-of-correlation functions using a final interrogation window size of 8×8 px computed from 24,000 double frame PIV images $2,560 \times 1,100$ px in size. The moments in the figure are normalized by the bulk velocity, which is the vertically averaged horizontal mean velocity component at $x = 0$.

The turbulent structures in the flow are of finite size, unlike the one in the previous simulations. Furthermore, the flow is well resolved, the PIV images are of good quality and the particle image density was relatively high. Thus, standard window correlation can capture a large fraction of the velocity fluctuations. The window-correlation results (not shown here) have the same overall structure as those using the deconvolution approach from Fig. 7. However, some of the higher order moments differ between the two approaches. So far it is unclear which of both methods reveals more accurate results. To identify the source of the remaining bias error more research is required. Two effects that are believed to be able to affect the accuracy are velocity gradients and image noise.

6. CONCLUSIONS

The developed approach, which estimates the velocity's PDF from the deconvolution of the discrete cross-correlation function and the auto-correlation function, was shown to be able to reliably estimate higher order moments. The comparison of the results achieved with standard window correlation, deconvolution of analytical fit functions and of the discrete correlation functions revealed that only the deconvolution of the discrete correlation functions can handle complex shaped PDFs with an asymmetric peak or two separated peaks. The investigation of the effect of different parameters by using synthetic PIV images allows to find optimized conditions. It was shown that the approach works well for a digital particle image diameter between 1.5 and 5 px. The image number has a strong impact on the random error of the estimated stresses. Depending on the order of the moment of interest and on the desired accuracy a few hundred up to several thousand PIV image pairs are required, which is easy to acquire and to evaluate with modern equipment.

The developed method is especially beneficial in the case of thin shear layers combined with low optical magnification, where the turbulent structures appear small compared to the interrogation window size that can be applied. Here, standard window correlation can only capture a fraction of the PDF due to spatial low-pass filtering, while the averaged correlation functions still contain the full PDF. The deconvolution approach is very general and can be applied to any averaged correlation function under the following conditions: (1) Cross-correlation and auto-correlation function must be sufficiently smooth for the deconvolution procedure, (2) cross-correlation and auto-correlation function must be computed with the same window weighting function and (3) the size of the correlation plane must be large enough to contain the full correlation functions, such that the full PDF can be extracted. To further increase the spatial resolution the method can be applied as well to correlation functions computed single-pixel ensemble-correlation.

In order to develop a tool that can be used in a standard PIV software, further investigations are needed to analyze the effect of image noise, the correlation window size, velocity gradients and other parameters on the accuracy of the estimated moments. Nevertheless, it was demonstrated that the approach has the potential to compensate for bias errors which occur by using standard evaluation tools.

ACKNOWLEDGMENTS

Financial support from the German Research Foundation in the framework of the TRR 40 is gratefully acknowledged by the authors. The analyzed data set was acquired with financial support from the European Community's Seventh Framework program (FP7/2007-2013) under grant agreement No. 265695.

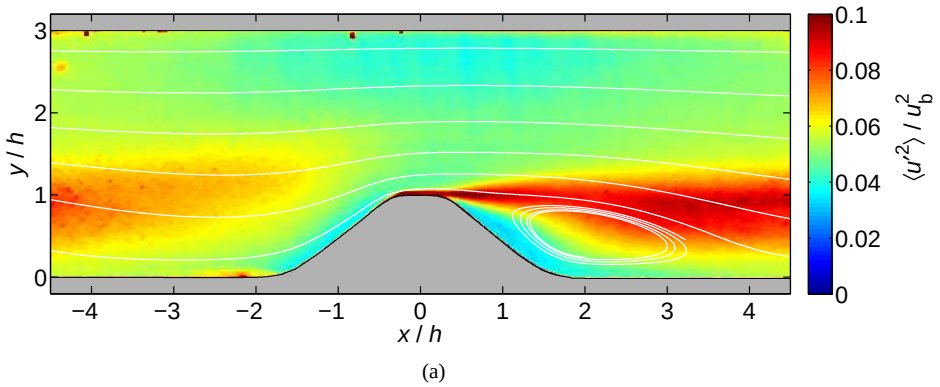

(a)

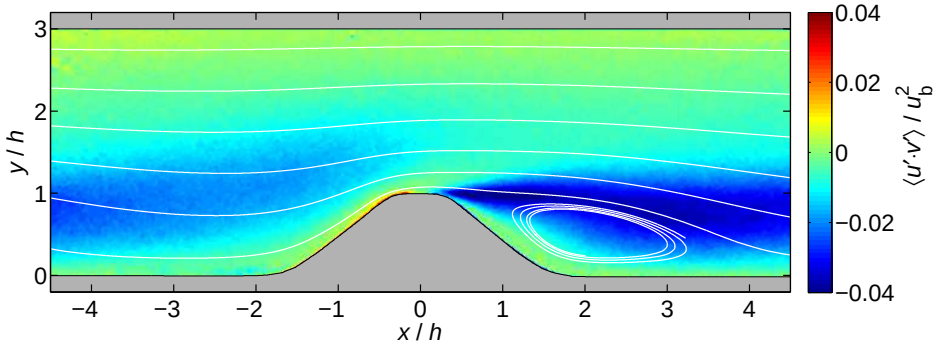

(b)

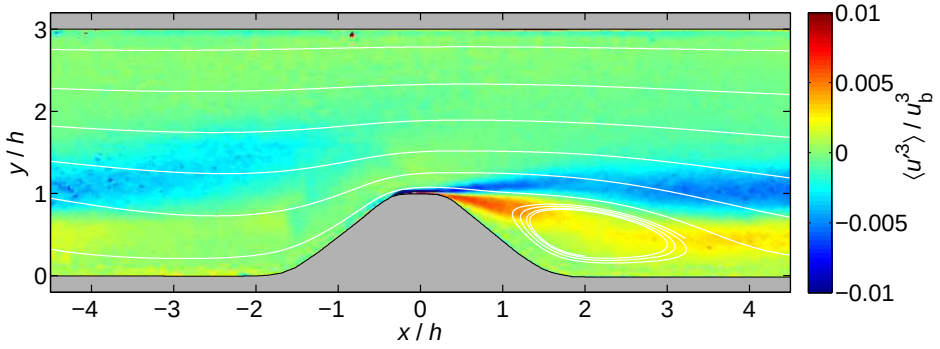

(c)

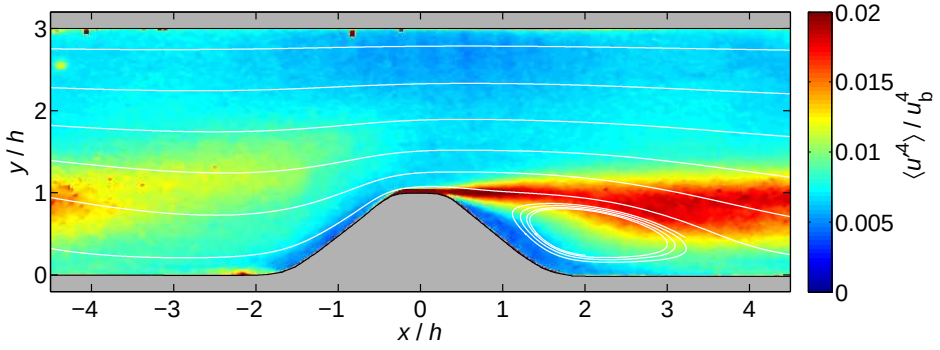

(d)

Figure 7: Exemplary moments of different order for a water flow over periodic hills at a Reynolds number of $\mathrm{Re_h} = 8,000$, based on the hill height.

REFERENCES

[1] R. J. Adrian. Double Exposure, Multiple-Field Particle Image Velocimetry for Turbulent Probability Density. *Opt and Laser Eng*, 9:211–228, 1988.

[2] W. Arnold, K. D. Hinsch, and D. Mach. Turbulence level measurement by speckle velocimetry. *Appl Optics*, 25:330–331, 1986.

[3] Christian Cierpka, Sven Scharnowski, Michael Manhart, , and Christian J. Kähler. On the significance of high spatial resolution to capture all relevant scales in the turbulent flow over periodic hills. In *10th International Symposium on Particle Image Velocimetry PIV13, Delft, The Netherlands, July 1-3*, 2013.

[4] C. J. Kähler, S. Scharnowski, and C. Cierpka. On the resolution limit of digital particle image velocimetry. *Exp Fluids*, 52:1629–1639, 2012.

[5] C. J. Kähler, S. Scharnowski, and C. Cierpka. On the uncertainty of digital PIV and PTV near walls. *Exp Fluids*, 52:1641–1656, 2012.

[6] C. D. Meinhart, S. T. Wereley, and J. G. Santiago. A PIV algorithm for estimating time-averaged velocity fields. *J Fluids Eng*, 122:285–289, 2000.

[7] C. Rapp and M. Manhart. Flow over periodic hills: an experimental study. *Exp Fluids*, 51:247–269, 2011.

[8] S. Scharnowski, R. Hain, and C. J. Kähler. Reynolds stress estimation up to single-pixel resolution using PIV-measurements. *Exp Fluids*, 52:985–1002, 2012.

[9] S. Scharnowski and C. J. Kähler. On the effect of curved streamlines on the accuracy of PIV vector fields. *Exp Fluids*, 54:1435, 2013.

[10] Julio Soria and Christian Willert. On measuring the joint probability density function of three-dimensional velocity components in turbulent flows. *Meas Sci Tech*, 23:065301, 2012.

[11] J. Westerweel, P. F. Geelhoed, and R. Lindken. Single-pixel resolution ensemble correlation for micro-PIV applications. *Exp Fluids*, 37:375–384, 2004.